GEOLOGY | THE GEOLOGICAL SOCIETY OF AMERICA®

https://doi.org/10.1130/G54551.1

Manuscript received 18 February 2026
Revised manuscript received 17 April 2026
Manuscript accepted 30 April 2026

Published online 15 May 2026

Microcontinent collision triggered Jurassic subduction transference in central Tibet

Anlin Ma[1,*], Zhiyong Yan[2,*], Xiumian Hu[1,#], Eduardo Garzanti[3], Taras Gerya[4], Alex Pullen[5], Robert J. Stern[6], and Wen Lai[7]

[1]State Key Laboratory of Critical Earth Material Cycling and Mineral Deposits, Key Laboratory of Surficial Geochemistry (Ministry of Education), School of Earth Sciences and Engineering, Nanjing University, Nanjing 210023, China
[2]College of Geophysics and Petroleum Resources, and Key Laboratory of Exploration Technologies for Oil and Gas Resources (Ministry of Education), Yangtze University, Wuhan 430100, China
[3]Department of Earth and Environmental Sciences, Università di Milano-Bicocca, Milano 20126, Italy
[4]Institute of Geophysics, Department of Earth and Planetary Sciences, Swiss Federal Institute of Technology (ETH Zurich), Sonneggstrasse 5, 8092 Zurich, Switzerland
[5]Department of Environmental Engineering and Earth Sciences, Clemson University, Clemson, South Carolina 29634, USA
[6]Department of Sustainable Earth Systems Sciences, University of Texas at Dallas, Richardson, Texas 75080, USA
[7]School of Geography and Environmental Engineering, Gannan Normal University, Ganzhou 341000, China

ABSTRACT

Subduction transference occurs when an existing subduction zone is choked by the arrival of buoyant crust, and a new subduction zone is generated on the down-going plate to accommodate continuing convergence. Although subduction transference triggered by microcontinent collision was conceptually proposed as a viable tectonic mechanism across several Tethyan oceanic branches, evidence remains controversial, and geodynamic controls are unclear. Here, we report geological data from central Tibet documenting the Early Jurassic northward subduction initiation of the Bangong-Nujiang Ocean, followed by collision with a presently ~70-km-wide microcontinent, ophiolite obduction, foreland-basin development, and initiation of a new north-dipping subduction zone to the south of the microcontinent in the late Middle to Late Jurassic. According to numerical geodynamic simulations, such a process can be triggered by an increase in buoyancy and/or lithospheric mantle strength of the collided microcontinent. Our study provides a geological example of subduction transference triggered by a narrow microcontinent collision, able to explain the progressive suturing of microcontinents in the Tethyan realm.

INTRODUCTION

Subduction initiation by transference was proposed as a mechanism for sustaining the progressive addition of microcontinents to Eurasia in the Mesozoic–earliest Cenozoic, leading to the multistage growth of the Himalayan-Tibetan orogen (Kapp and DeCelles, 2019; Zhong and Li, 2020; Metcalfe, 2021). However, any convincing application of this model must withstand geological scrutiny concerning pre-collisional paleogeography, timing of continent collision and subduction initiation, and subduction polarity (e.g., Li and Robinson, 2023; Ma et al., 2025). This is particularly true for the closure of the Bangong-Nujiang Ocean to form the Bangong-Nujiang suture zone in central Tibet (Fig. 1A), as the onset of oceanic subduction has been controversially inferred as either Triassic or Jurassic in age, with final oceanic closure in the late Middle Jurassic or early Late Cretaceous (e.g., Zhu et al., 2016; Hu et al., 2022).

The Dongqiao-Beila area of the Bangong-Nujiang suture zone in central Tibet preserves a presently narrow (70-km-wide) Dongkaco microcontinent (Ma et al., 2024), where the model of subduction transference induced by microcontinent collision can be tested. From north to south, tectonic units include the Qiangtang block, Amdo-Qixiangco ophiolite, Gacangjian arc, Zigetangco basin, Dongqiao ophiolite, Dongkaco microcontinent, Beila basin, Daruco arc, Beila ophiolite, and Lhasa block (Figs. 1B–1D and Fig. S1 in the Supplemental Material[1]). The Dongkaco microcontinent is delimited by the Dongqiao and Beila suture zones and includes Upper Paleozoic passive-margin strata similar to those in the Lhasa block (Fig. 1C; Ma et al., 2024). Previous studies suggested that the Amdo-Qixiangco, Dongqiao, and Beila ophiolites formed at 188–184 Ma, 190–181 Ma, and 177–148 Ma, respectively (Hu et al., 2022; Zhai et al., 2024), and Daruco arc rocks at 166–160 Ma (Zeng et al., 2016; Li et al., 2020). However, the age of the Gacangjian arc and the age, provenance, and tectonic setting of deep-marine sedimentary rocks in the Zigetangco, Beila, and northern Lhasa basins have not been systematically investigated. Consequently, competing tectonic models, including microcontinent collision or accretion, oceanic-plateau collision, and active oceanic-ridge collision, were all proposed to explain the Late Jurassic interactions with the Qiangtang block (Girardeau et al., 1984; Li et al., 2020; Yan and Zhang, 2020; Hu et al., 2022).

Xiumian Hu https://orcid.org/0000-0002-5401-8682
*These authors contributed equally to this work.
#Corresponding author: huxm@nju.edu.cn

[1]Supplemental Material. Analytical methods, numerical geodynamic simulation methods, complied data sources, Figures S1–S8, and Tables S1–S8. Please visit https://doi.org/10.1130/GEOL.S.32194071 to access the supplemental material; contact editing@geosociety.org with any questions.

CITATION: Ma, A., et al., 2026, Microcontinent collision triggered Jurassic subduction transference in central Tibet: Geology, v. XX, p. , https://doi.org/10.1130/G54551.1

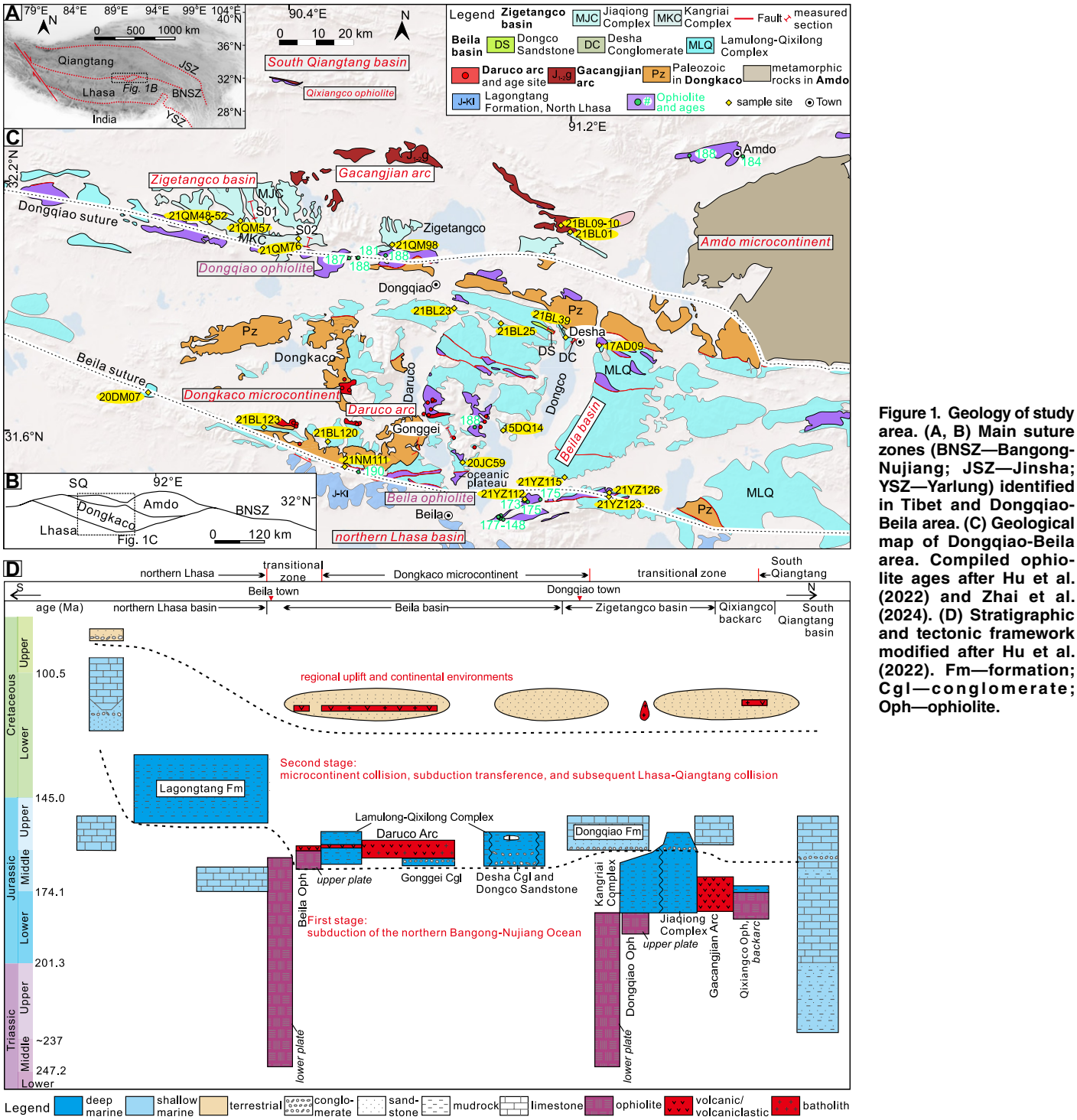

Figure 1. Geology of study area. (A, B) Main suture zones (BNSZ—Bangong-Nujiang; JSZ—Jinsha; YSZ—Yarlung) identified in Tibet and Dongqiao-Beila area. (C) Geological map of Dongqiao-Beila area. Compiled ophiolite ages after Hu et al. (2022) and Zhai et al. (2024). (D) Stratigraphic and tectonic framework modified after Hu et al. (2022). Fm—formation; Cgl—conglomerate; Oph—ophiolite.

Other continental suturing models include microcontinent subduction without accretion, microcontinent accretion, and subduction polarity reversal (Cloos, 1993; van Hinsbergen and Schouten, 2021). Previous numerical simulation studies considered the existence of a weak detachment within the crust, its depth, microcontinent's rheological strength, and convergence velocities, all factors that determine the fate of the subducting microcontinent (Tetreault and Buiter, 2012; Cui and Li, 2024). However, a systematic reevaluation of other key geodynamic parameters (e.g., width and crustal thickness of the collided terrane and density of oceanic lithosphere) was not conducted. Here, we provide geological, geochemical, and geochronological data on the volcanic arcs and Jurassic sedimentary basins in the Dongqiao-Beila area, which, combined with geodynamic simulations, allow us to evaluate whether subduction transference could have occurred in the Bangong-Nujiang Ocean and to discuss the implications for the geodynamic evolution of the Tethyan realm.

METHODS, RESULTS, AND INTERPRETATIONS

All analytical methods, including sandstone petrology, zircon U-Pb geochronology and hafnium and oxygen isotopes, volcanic rock and Cr-spinel geochemistry, and numerical geodynamic simulation, are described in the Supplemental Material.

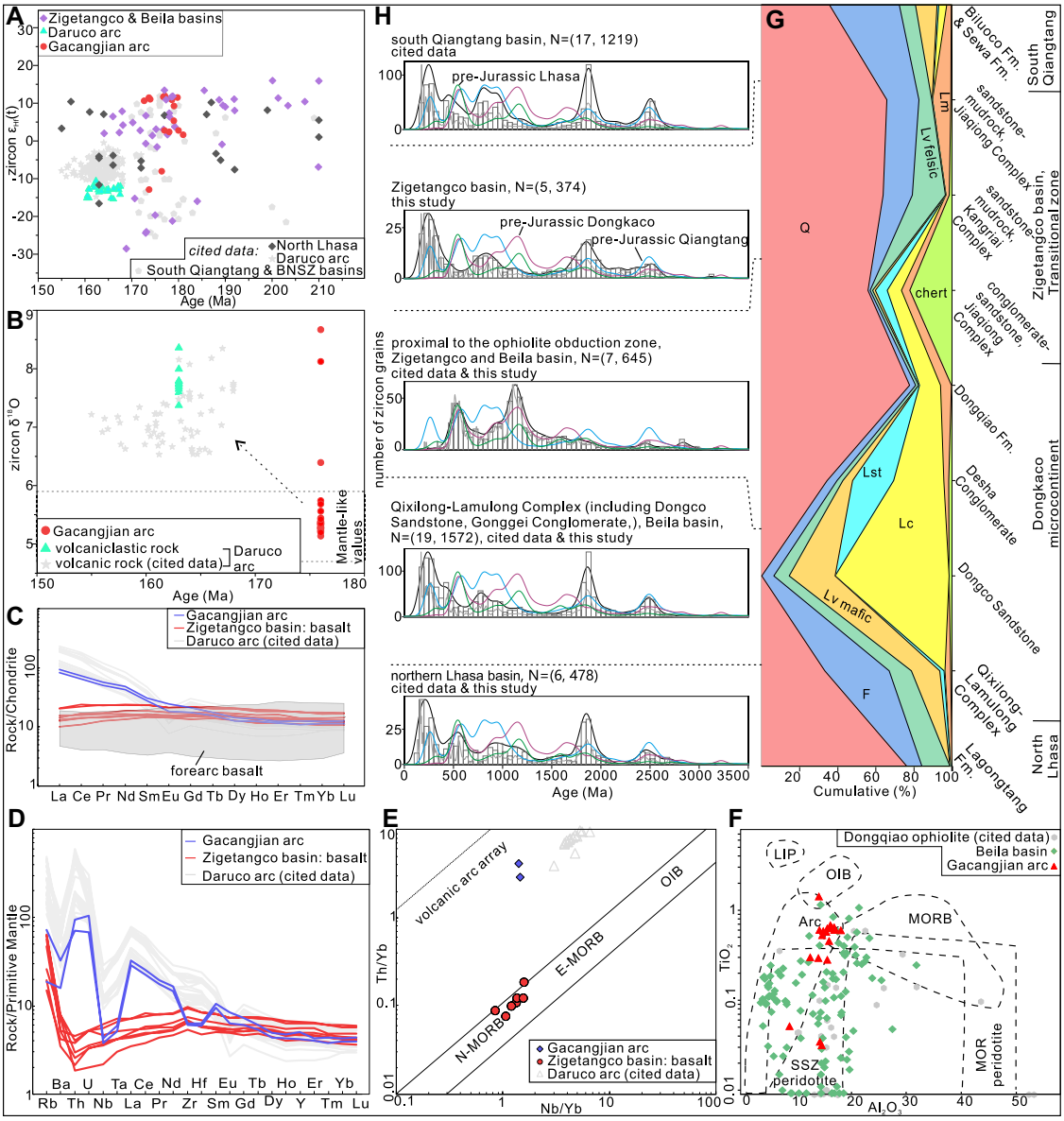

Figure 2. Geological and geochemical data. (A) Zircon $\varepsilon_{Hf}(t)$ values vs. U-Pb ages; (B) zircon $\delta^{18}O$ vs. U–Pb ages; (C, D) rare earth element patterns and trace-element spider diagrams for basalt in Zigetangco basin and Gacangjian arc volcanic rocks; (E) Nb/Yb vs. Th/Yb discrimination diagram (Pearce, 2008); (F) discrimination of detrital Cr-spinel provenance using TiO_2 vs. Al_2O_3 diagram (Kamenetsky et al., 2001); (G) petrographic composition of sandstones from South Qiangtang to North Lhasa: Q (quartz), F (feldspar), L (lithics: Lc—limestone; Lst—siliciclastic; Lm—metamorphic; Lv—volcanic); (H) kernel density estimation (black line), probability density plot (gray line), and histograms of detrital-zircon U-Pb ages. BNSZ—Bangong-Nujiang suture zone; LIP—large igneous province; MOR—mid-oceanic ridge; MORB—mid-oceanic-ridge basalt; N-MORB—normal MORB; E-MORB—enriched MORB; OIB—ocean-island basalt; SSZ—supra-subduction zone.

Gacangjian Arc

U-Pb dating of zircons from a tuff sample of the Gacangjian arc and from an exotic rhyolite block in the Beila basin, inferred to have been sourced from the Gacangjian arc, yielded the same weighted mean age of 176 Ma. These zircons have $\varepsilon_{Hf}(t)$ values between +1.6 and +12 (Fig. 2A), and $\delta^{18}O$ mainly between 5.1‰ and 5.7‰ (averaging ~5.3‰), indicative of mantle origin (Valley et al., 2005; Fig. 2B).

Two volcanic rocks from the Gacangjian arc, containing 42.65 and 56.05 wt% SiO_2, enriched in light rare earth elements (Fig. 2C) and large-ion-lithophile elements and depleted in high-field-strength elements (Fig. 2D), plot in the volcanic-arc array field in the Th/Yb versus Nb/Yb diagram (Fig. 2E; Pearce, 2008). Cr-spinels from the tuff sample, containing 0.3–0.8 wt% TiO_2 and <18 wt% Al_2O_3, plot mainly in the magmatic-arc field (Fig. 2F; Kamenetsky et al., 2001).

Daruco Arc

Two samples of volcaniclastic rocks yielded weighted mean zircon U-Pb ages of 165–163 Ma, with zircons $\varepsilon_{Hf}(t)$ values from −15 to −10 (Fig. 2A), more negative than those of Daruco-arc magmatic rocks [$\varepsilon_{Hf}(t)$ from −12 to −2; Zeng et al., 2016; Li et al., 2020]. The zircon $\delta^{18}O$ values range from 7.4‰ to 8.4‰ (average 7.8‰), similar to Daruco arc magmatic rocks (ranging from 6.5‰ to 8.4‰, average 7.2‰; Fig. 2B; Hu et al., 2020; Li et al., 2020).

Zigetangco Basin

Deposition in the deep-marine Zigetangco basin started with mudrock interbedded with basalt (S02 section, Fig. S2). Seven basalt samples exhibit flat chondrite-normalized rare earth element patterns (Fig. 2C) and plot close to the normal mid-oceanic-ridge basalt (N-MORB) field in the Th/Yb versus Nb/Yb diagram (Fig. 2E). The mudrock-sandstone couplets of the Jiaqiong Complex were deposited in the proximal northern part of the basin, whereas mudrocks and a few sandstones of the Kangriai Complex characterize the distal southern part. Sandstones from the Jiaqiong and Kangriai complexes are quartzose (Fig. 2G), and their maximum depositional ages (MDAs) become younger up-section from 210 Ma to 180–170 Ma (Table S1). The Jurassic zircons yielded both positive (+2 to +12) and negative $\varepsilon_{Hf}(t)$ values (−8 to −28), implying contribution from the continental Gacangjian arc and Qiangtang block to the north (Fig. 2A; Ma et al., 2023).

The uppermost part of the Jiaqiong Complex (S01 section, Fig. S2) consists of proximal deep-sea fan channelized conglomerates. Pebbles and lithic fragments consist of sandstone, limestone, and chert (Fig. 2G). The detrital zircons yielded MDAs of 513–337 Ma, and U-Pb age spectra compare well with rock of the Dongkaco and

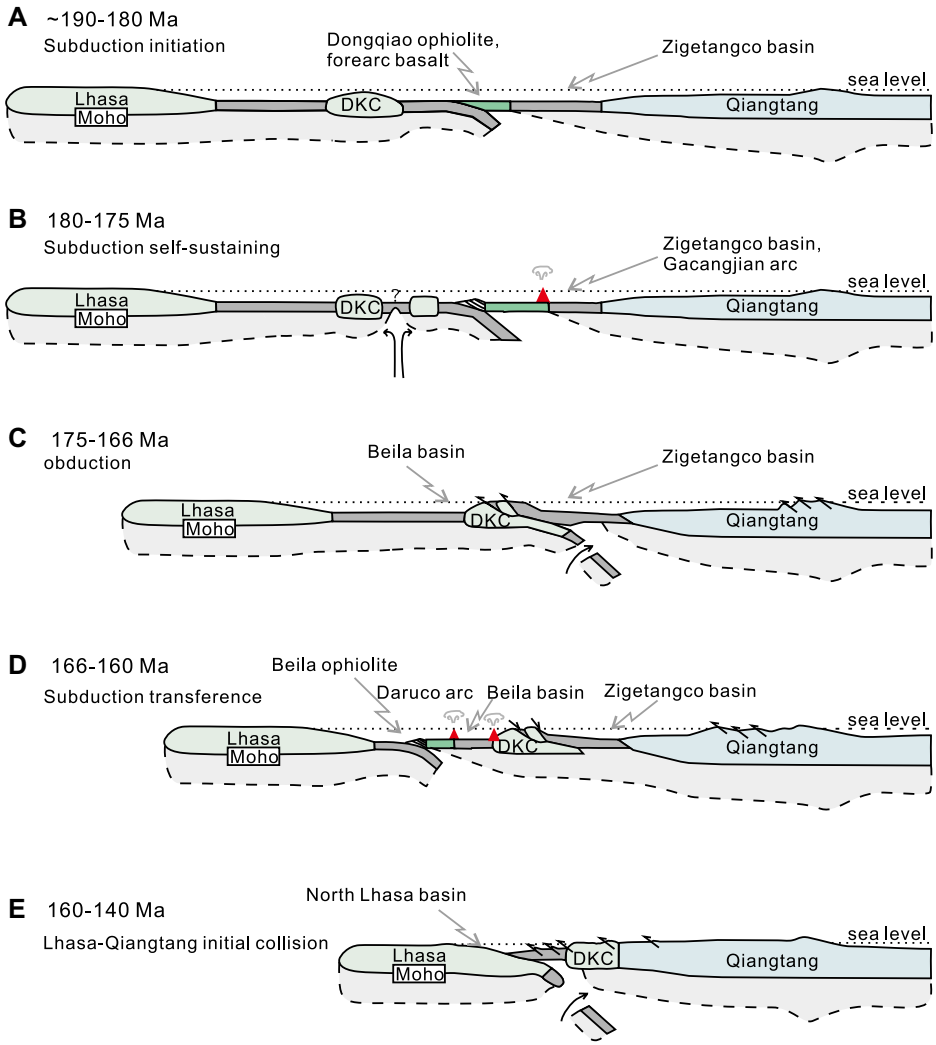

Figure 3. Tectonic reconstruction based on geological data. (A, B) Northward subduction of the Bangong-Nujiang Ocean (BNO) northern branch initiated at ca. 190 Ma, generating Dongqiao arc-trench system by ca. 175 Ma; (C) subduction of Dongkaco microcontinent (DKC) beneath Dongqiao forearc caused obduction of arc-trench system at ca. 175–166 Ma; (D) northward subduction of southern BNO branch initiated by transference at ca. 166–160 Ma; (E) initial Lhasa-Qiangtang collision led to development of North Lhasa foreland basin. Oceanic crust in gray (green if newly generated). The dashed line marks the base of the mantle lithosphere.

Lhasa but poorly with those of the South Qiangtang (Fig. 2H).

Beila Basin

The internally coherent Desha Conglomerate in the deep-marine Beila basin (Desha section, Fig. S2) comprises quartzo-lithic sandstones (Figs. 2G, S3, and S4) and conglomerates with pebbles mainly consisting of sandstone, limestone, basalt, and peridotite. U-Pb ages of detrital zircons mostly range between 1200 Ma and 513 Ma, indicating affinity with the Dongkaco and Lhasa terranes (Figs. 2H and S5).

The Dongco Sandstone consists of alternating sandstone and mudrock, locally with limestone olistoliths (West Desha section, Fig. S2) containing Late Jurassic corals (Fig. S6) sourced from the Dongqiao Formation to the north (Ma et al., 2020). Sandstones are mainly lithic (Fig. 2G), and detrital zircons yielded U-Pb ages of Qiangtang affinity, with an MDA of 185 Ma.

Sandstones in the Gonggei Conglomerate and Lamulong-Qixilong Complex contain more feldspar (Fig. 2G), and their zircon U-Pb age spectra display Qiangtang affinities (Fig. 2H). Three tuff samples yielded weighted mean zircon U-Pb ages of 173–169 Ma, and the Gonggei Conglomerate is stratigraphically overlain by 165–163 Ma tuffs (Figs. S1 and S2). The MDAs of 12 samples range from 215 Ma to 166 Ma.

Latest Triassic to Jurassic zircons in the Beila basin yielded $\varepsilon_{Hf}(t)$ values mainly between +2 and +16 and subordinately between −8 and −28 (Fig. 2A). Detrital Cr-spinels with TiO_2 <1 wt% mainly plot in the field of supra-subduction-zone mantle rocks, similar to Cr-spinels from the Dongqiao ophiolite (Fig. 2F). Some Cr-spinels plot in the MORB and magmatic-arc fields (Fig. 2F).

DISCUSSION AND CONCLUSIONS

Geological Evolution

The N-MORB–like geochemistry of basalt at the base of the Zigetangco basin suggests a magma source unaffected by fluids derived from the subducting slab, resembling forearc basalt generated through mantle decompression melting and near-trench spreading during the earliest stages of subduction (Whattam and Stern, 2011; Reagan et al., 2023). As the interbedded siltstone lacks Middle Jurassic magmatic arc-derived zircons and yielded an MDA of ca. 225 Ma, the basalt should be latest Triassic to Early Jurassic in age. Once the subduction became self-sustained at 190–180 Ma, the Dongqiao arc-trench system formed, including rocks of the Dongqiao ophiolite, Zigetangco forearc basin, ca. 175 Ma Gacangjian arc, and possibly back-arc Qixiangco-Amdo ophiolite (Figs. 3A and 3B).

Subsequently, plate convergence drove the Dongkaco microcontinent to the trench, inducing obduction of the arc-trench system over the microcontinent (Fig. 3C). This occurred earlier than the deposition of the subaerial to shallow-marine syn-orogenic Dongqiao Formation (ca. 164–152 Ma; Girardeau et al., 1984; Ma et al., 2020) and of the deep-marine Jiaqiong Complex and Desha Conglomerate. The Dongco Sandstone, Gonggei Conglomerate, and Qixilong-Lamulong Complex in the Beila basin were also sourced from the obducted ophiolites and accretionary prism.

Microcontinent collision also induced subduction initiation of the southern Bangong-Nujiang Ocean branch (Fig. 3D). In the Beila suture, forearc basalts pass stratigraphically upward to boninitic dikes and boninites dated as 164 Ma (Yan and Zhang, 2020; Tang et al., 2021), a succession analogous to proto-forearc sequences in the Izu-Bonin-Mariana system (Reagan et al., 2023). As the Daruco arc is located to the north of the Beila ophiolite, the subduction of the southern Bangong-Nujiang Ocean was north-dipping, rather than south-dipping (Yang et al., 2021). Although the southern Bangong-Nujiang Ocean was interpreted to subduct southward because the Gajia mélange was believed to receive detritus from the Lhasa block (Lai et al., 2017), the sediments can be alternatively interpreted as derived from the north (Hu et al., 2022).

The northward polarity of both Dongqiao and Beila subduction systems rules out a polarity-reversal model. A model involving a single retreating subduction zone is also not favored because: (1) the Dongqiao ophiolite-Gacangjian arc and the Beila ophiolite-Daruco arc formed in distinct episodes and in different places, not in a continuous process (Hu et al., 2022); and (2) the forearc basalt suggests subduction initia-

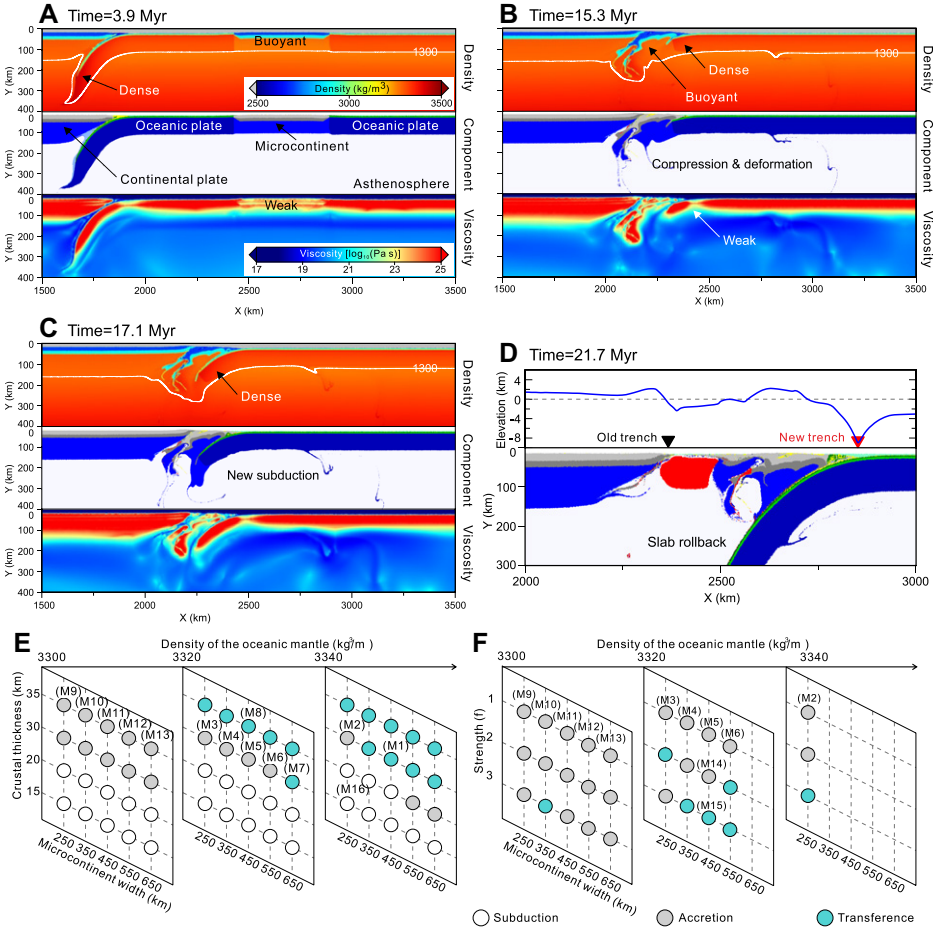

Figure 4. Numerical model. Panels A–D illustrate model M1: (A) Oceanic plate carries a microcontinent that begins to subduct along the initial weak zone, corresponding to Figure 3A; (B) microcontinent resists subduction at 15.3 m.y., corresponding to Figure 3C; (C) new subduction zone forms behind microcontinent at 17.1 m.y., corresponding to Figure 3D; (D) magnified image showing evolution of new subduction zone at 21.7 m.y., with surface elevation shown above; (E, F) sensitivity of results to variation of microcontinent's width, crustal thickness, density of oceanic mantle lithosphere, and strength of microcontinent lithospheric mantle.

tion in the Beila suture (Yan and Zhang, 2020; Tang et al., 2021). The oceanic plateau collision model is also not favored because: (1) oceanic plateau's fragments are limited in areal extent (Fig. 1C; Zhang et al., 2021); and (2) detrital spinels with high Ti content, indicative of oceanic plateau provenance, are rare in Jurassic sedimentary rocks of the Beila basin (Fig. 2F).

Finally, the Lhasa block collided with the Dongkaco-Qiangtang block at 160–140 Ma (Fig. 3E). The Upper Jurassic to Lower Cretaceous Lagongtang Formation is considered as deposited in a foreland basin on the North Lhasa terrane, as it received detritus from rocks of South Qiangtang affinity, Dongkaco microcontinent, and Daruco arc, as indicated by detrital zircon U-Pb age peaks and zircon $\varepsilon_{Hf}(t)$ values from 0 to −5 (Figs. 2A and 2H).

Geodynamic Implications

We conducted geodynamic simulations to reproduce the observation-based tectonic evolution and to systematically test the key parameters that control the fate of a microcontinental block. Among the 68 simulations, model M1 best reproduces the subduction transference process as reconstructed from geologic data (Figs. 4A–4D). The results suggest that high density of the oceanic mantle lithosphere (>3.32 g/cm^3), microcontinent's width (>250 km), crustal thickness (>30 km), and strength of mantle lithosphere (*f*-factor >2) all promote resistance to microcontinent subduction, thus favoring subduction-zone transference (Figs. 4E and 4F). The *f*-factor is a model parameter used to describe the mechanical strength of the lithospheric mantle, higher values meaning greater resistance to deformation (Xiang et al., 2024). Considering >47% upper crustal shortening (Kapp et al., 2007), the width of the Dongkaco microcontinent in the Early Cretaceous may have exceeded 130 km. Additional convergence may have resulted from subduction of Dongkaco continental crust, as inferred for initial underthrusting of India beneath Asia (Wang et al., 2022). Regardless, the Dongkaco microcontinent was much narrower than the Lhasa block from which it was rifted (Ma et al., 2024).

In a broader view, ribbon-like continents with much wider and thicker crust than the Dongkaco should be more prone to induce subduction transference. The collision between the Qiangtang block and Eurasia during the Middle to Late Triassic, therefore, may have triggered the northward subduction of the Bangong-Nujiang Ocean in the Late Triassic to earliest Jurassic. The latest Jurassic Lhasa-Qiangtang collision may have triggered reinitiation of subduction in the southern Yarlung branch of the Neo-Tethys Ocean (Kapp and DeCelles, 2019; Zhang et al., 2019). Similar processes may have taken place in other long-lived convergent systems where buoyant continental fragments enter active trenches.

ACKNOWLEDGMENTS

This work is supported by the National Natural Science Foundation of China (grants 42488201 and 42472161). This is University of Texas at Dallas contribution #1739. Gerya acknowledge support by Swiss National Science Foundation (SNSF) research projects 200021-231594 and 200021_192296. We thank Rob Strachan for editorial handling and Delores M. Robinson, Andrew Laskowski, and one anonymous reviewer for their constructive comments.

REFERENCES CITED

Cloos, M., 1993, Lithospheric buoyancy and collisional orogenesis: Subduction of oceanic plateaus, continental margins, island arcs, spreading ridges, and seamounts: Geological Society of America Bulletin, v. 105, p. 715–737, https://doi.org/10.1130/0016-7606(1993)105<0715:LBACOS>2.3.CO;2.

Cui, F., and Li, Z.H., 2024, Terrane collision-induced subduction initiation: Mode selection and implications for western Pacific subduction system: Geochemistry, Geophysics, Geosystems, v. 25, https://doi.org/10.1029/2023GC011155.

Girardeau, J., Marcoux, J., Allegre, C.J., Bassoullet, J.P., Tang, Y.K., Xiao, X.C., Zao, Y.G., and Wang, X.B., 1984, Tectonic environment and geodynamic significance of the Neo-Cimmerian Donqiao ophiolite, Bangong-Nujiang suture zone, Tibet: Nature, v. 307, p. 27–31, https://doi.org/10.1038/307027a0.

Hu, W.-L., Wang, Q., Yang, J.-H., Tang, G.-J., Qi, Y., Ma, L., Yang, Z.-Y., and Sun, P., 2020, Amphibole and whole-rock geochemistry of early Late Jurassic diorites, Central Tibet: Implications for petrogenesis and geodynamic processes: Lithos, v. 370–371, https://doi.org/10.1016/j.lithos.2020.105644.

Hu, X.-M., Ma, A.-L., Xue, W.-W., Garzanti, E., Cao, Y., Li, S.-M., Sun, G.-Y., and Lai, W., 2022, Exploring a lost ocean in the Tibetan Plateau: Birth, growth, and demise of the Bangong-Nujiang Ocean: Earth-Science Reviews, v. 229, https://doi.org/10.1016/j.earscirev.2022.104031.

Kamenetsky, V.S., Crawford, A.J., and Meffre, S., 2001, Factors controlling chemistry of magmatic spinel: An empirical study of associated olivine, Cr-spinel and melt inclusions from primitive rocks: Journal of Petrology, v. 42, p. 655–671, https://doi.org/10.1093/petrology/42.4.655.

Kapp, P., and DeCelles, P.G., 2019, Mesozoic–Cenozoic geological evolution of the Himalayan-Tibetan orogen and working tectonic hypotheses: American Journal of Science, v. 319, p. 159–254, https://doi.org/10.2475/03.2019.01.

Kapp, P., DeCelles, P.G., Gehrels, G.E., Heizier, M., and Ding, L., 2007, Geological records of the Lhasa-Qiangtang and Indo-Asian collisions in the Nima area of central Tibet: Geological Society of America Bulletin, v. 119, p. 917–933, https://doi.org/10.1130/B26033.1.

Lai, W., Hu, X., Zhu, D., An, W., and Ma, A., 2017, Discovery of the early Jurassic Gajia mélange in the Bangong–Nujiang suture zone: Southward subduction of the Bangong–Nujiang Ocean?: International Journal of Earth Sciences, v. 106, p. 1277–1288, https://doi.org/10.1007/s00531-016-1405-1.

Li, S.M., Wang, Q., Zhu, D.C., Cawood, P.A., Stern, R.J., Weinberg, R., Zhao, Z., and Mo, X.X., 2020, Reconciling orogenic drivers for the evolution of the Bangong-Nujiang Tethys during Middle-Late Jurassic: Tectonics, v. 39, https://doi.org/10.1029/2019TC005951.

Li, Y., and Robinson, D.M., 2023, The India-Asia collision results from two possible pre-collisional crustal configurations of northern Greater India: Earth and Planetary Science Letters, v. 610, https://doi.org/10.1016/j.epsl.2023.118098.

Ma, A., Hu, X.-M., Kapp, P., BouDagher-Fadel, M., and Lai, W., 2020, Pre-Oxfordian (>163 Ma) ophiolite obduction in Central Tibet: Geophysical Research Letters, v. 47, https://doi.org/10.1029/2019GL086650.

Ma, A., Hu, X., Garzanti, E., Boudagher-Fadel, M., Xue, W., Han, Z., and Wang, P., 2023, Paleogeographic and tectonic evolution of Mesozoic Qiangtang basins (Tibet): Tectonophysics, v. 862, https://doi.org/10.1016/j.tecto.2023.229957.

Ma, A., Hu, X., Li, X., Pullen, A., Garzanti, E., and Suzuki, N., 2024, Timing of rifting of the Dongkaco microcontinent (Central Tibet) and implications for Neo-Tethyan evolution: Palaeogeography, Palaeoclimatology, Palaeoecology, v. 638, https://doi.org/10.1016/j.palaeo.2024.112054.

Ma, Y., Dekkers, M.J., Duarte, J.C., and Kusky, T., 2025, Subduction transference drove the Mesozoic convergence of microcontinents from Gondwana to Asia: Communications Earth & Environment, v. 6, 442, https://doi.org/10.1038/s43247-025-02410-1.

Metcalfe, I., 2021, Multiple Tethyan ocean basins and orogenic belts in Asia: Gondwana Research, v. 100, p. 87–130, https://doi.org/10.1016/j.gr.2021.01.012.

Pearce, J.A., 2008, Geochemical fingerprinting of oceanic basalts with applications to ophiolite classification and the search for Archean oceanic crust: Lithos, v. 100, p. 14–48, https://doi.org/10.1016/j.lithos.2007.06.016.

Reagan, M.K., Pearce, J.A., Shervais, J.W., and Christeson, G.L., 2023, Subduction initiation as recorded in the Izu-Bonin-Mariana forearc: Earth-Science Reviews, v. 246, https://doi.org/10.1016/j.earscirev.2023.104573.

Tang, Y., Zhai, Q.-G., Hu, P.-Y., Wang, W., Yan, Z., Wang, H.-T., and Zhu, Z.-C., 2021, Forearc lava stratigraphy of the Beila Ophiolite, north-central Tibetan Plateau: Magmatic response to initiation of subduction of the Bangong-Nujiang Meso-Tethys Ocean: Palaeogeography, Palaeoclimatology, Palaeoecology, v. 582, https://doi.org/10.1016/j.palaeo.2021.110663.

Tetreault, J.L., and Buiter, S.J.H., 2012, Geodynamic models of terrane accretion: Testing the fate of island arcs, oceanic plateaus, and continental fragments in subduction zones: Journal of Geophysical Research: Solid Earth, v. 117, https://doi.org/10.1029/2012JB009316.

Valley, J.W., et al., 2005, 4.4 billion years of crustal maturation: Oxygen isotope ratios of magmatic zircon: Contributions to Mineralogy and Petrology, v. 150, p. 561–580, https://doi.org/10.1007/s00410-005-0025-8.

van Hinsbergen, D.J., and Schouten, T.L., 2021, Deciphering paleogeography from orogenic architecture: Constructing orogens in a future supercontinent as thought experiment: American Journal of Science, v. 321, p. 955–1031, https://doi.org/10.2475/06.2021.09.

Wang, Y., Zhang, L., and Li, Z.-H., 2022, Metamorphic densification can account for the missing felsic crust of the Greater Indian continent: Communications Earth & Environment, v. 3, 166, https://doi.org/10.1038/s43247-022-00493-8.

Whattam, S.A., and Stern, R.J., 2011, The 'subduction initiation rule': A key for linking ophiolites, intra-oceanic forearcs, and subduction initiation: Contributions to Mineralogy and Petrology, v. 162, p. 1031–1045, https://doi.org/10.1007/s00410-011-0638-z.

Xiang, X., Chen, H., Chen, L., Xu, X., Lin, X., Li, Z., and Yan, Z., 2024, Plume-modified lithosphere mantle controlled the Cenozoic sediment thickness in the Tarim Basin: Geophysical Research Letters, v. 51, https://doi.org/10.1029/2023GL106203.

Yan, L.-L., and Zhang, K.-J., 2020, Infant intra-oceanic arc magmatism due to initial subduction induced by oceanic plateau accretion: A case study of the Bangong Meso-Tethys, central Tibet, western China: Gondwana Research, v. 79, p. 110–124, https://doi.org/10.1016/j.gr.2019.08.008.

Yang, Z.-Y., Tang, J.-X., Zhang, K.-J., Zhao, X.-Y., Li, H.-F., Wang, Y., Li, F.-Q., Ran, F.-Q., and Huang, Y.-R., 2021, Southward subduction of the Bangong–Nujiang oceanic lithosphere triggered back-arc spreading: Evidence from the Late Jurassic Kongnongla magnesian andesites in central Tibet: Lithos, v. 398–399, https://doi.org/10.1016/j.lithos.2021.106250.

Zeng, Y.-C., Chen, J.-L., Xu, J.-F., Wang, B.-D., and Huang, F., 2016, Sediment melting during subduction initiation: Geochronological and geochemical evidence from the Darutso high-Mg andesites within ophiolite mélange, central Tibet: Geochemistry, Geophysics, Geosystems, v. 17, p. 4859–4877, https://doi.org/10.1002/2016GC006456.

Zhai, Q., Tang, Y., Hu, P., Liu, Y., and Wang, W., 2024, Induced subduction initiation near an ultra-slow spreading ridge: A case study from the Beila ophiolite in the north-central Tibetan Plateau: Gondwana Research, v. 135, p. 1–16, https://doi.org/10.1016/j.gr.2024.07.019.

Zhang, C., Liu, C.-Z., Xu, Y., Ji, W.-B., Wang, J.-M., Wu, F.-Y., Liu, T., Zhang, Z.-Y., and Zhang, W.-Q., 2019, Subduction re-initiation at dying ridge of Neo-Tethys: Insights from mafic and metamafic rocks in Lhaze ophiolitic mélange, Yarlung-Tsangbo Suture Zone: Earth and Planetary Science Letters, v. 523, 115707, https://doi.org/10.1016/j.epsl.2019.07.009.

Zhang, W.-Q., Liu, C.-Z., Liu, T., Zhang, C., and Zhang, Z.-Y., 2021, Subduction initiation triggered by accretion of a Jurassic oceanic plateau along the Bangong–Nujiang Suture in central Tibet: Terra Nova, v. 33, p. 150–158, https://doi.org/10.1111/ter.12500.

Zhong, X., and Li, Z.H., 2020, Subduction initiation during collision-induced subduction transference: Numerical modeling and implications for the Tethyan evolution: Journal of Geophysical Research: Solid Earth, v. 125, https://doi.org/10.1029/2019JB019288.

Zhu, D.-C., Li, S.-M., Cawood, P.A., Wang, Q., Zhao, Z.-D., Liu, S.-A., and Wang, L.-Q., 2016, Assembly of the Lhasa and Qiangtang terranes in central Tibet by divergent double subduction: Lithos, v. 245, p. 7–17, https://doi.org/10.1016/j.lithos.2015.06.023.

Printed in the USA